Aalborg Universitet

AALBORG UNIVERSITY

DENMARK

A Power Angle Limiting Method for Improving Stability of Grid-Forming Inverter Under Overcurrent Condition

Huang, Liang; Wu, Chao; Zhou, Dao; Blaabjerg, Frede

A Power Angle Limiting Method for Improving Stability of Grid-Forming Inverter Under Overcurrent Condition

Liang Huang
AAU Energy
Aalborg University
Aalborg, Denmark
lihu@energy.aau.dk

Chao Wu
Electrical Engineering
Shanghai Jiaotong University
Shanghai, China
wuchao@sjtu.edu.cn

Dao Zhou
AAU Energy
Aalborg University
Aalborg, Denmark
zda@energy.aau.dk

Frede Blaabjerg
AAU Energy
Aalborg University
Aalborg, Denmark
fbl@energy.aau.dk

Abstract—For conventional grid-following inverters, the overcurrent protection can be fulfilled easily by using the current reference limiting method. However, when this method is used for grid-forming (GFM) inverters, it may jeopardize the stability, because the power synchronization control law is destroyed when the current limit is triggered. To address this problem, this paper proposes a power angle limiting method used for the virtual-admittance-based GFM inverters, which can properly limit the output power and current of the inverters. Since limiting the power angle is more reasonable than directly limiting the current, the stability can be improved by using the proposed method. Detailed implementation of the proposed method is illustrated in this paper. Besides, the effectiveness of the proposed method is verified by the time-domain simulation.

Keywords—grid-forming inverter, virtual admittance, stability, power angle limit, overcurrent conditions

I. INTRODUCTION

Nowadays, grid-following (GFL) inverters have been widely used in renewable energy generation systems, such as wind and solar photovoltaic (PV) power plants. However, as the penetration of renewable energy increases, conventional GFL inverters with current source characteristics may not fully meet grid codes requirements [1]. Therefore, an alternative technique which is called "grid-forming" (GFM) inverter has been proposed in recent years. Since the GFM inverters have similar voltage source characteristics as the traditional synchronous generators (SGs) [2], they are deemed as promising solutions for the future power grid with a high percentage of renewable energy sources.

So far, many different GFM control schemes have been proposed [3]-[5], which can be generally divided into two categories. One is without an inner current control loop, while the other is with an inner current control loop (e.g. dual-loop voltage/current vector control) [6]. Because including the inner current control loop can reduce the voltage and current harmonics, the second category of GFM inverters with an inner current control loop attracts more research attention [7]. Moreover, a virtual impedance or admittance is usually used for the dual-loop GFM control scheme to improve the small-signal stability [8].

Based on existing studies [8], [9], it is known that the small-signal stability of the virtual-admittance-based GFM inverter is already acceptable under normal conditions. Specifically, when the value of virtual admittance is designed properly, the system is always stable within a wide range of short-circuit ratios (SCRs) [8]. Thus, no matter whether the grid is strong or weak, the virtual-admittance-based GFM inverter has good stability and robustness.

However, GFM inverters suffer from instability problems under abnormal conditions. Namely, when the current exceeds the rated range and triggers the overcurrent protection, existing overcurrent protection methods have some limitations. A typical current limiting method is the current reference limiting method [10], which has been successfully applied in the conventional GFL inverters. However, when this method is used for GFM inverters, it may worsen the synchronization stability because the power angle equation is not satisfied anymore when the current limit is triggered [11]. To address this problem, an easy way is to switch the control mode from the GFM control mode to the GFL control mode when the current limit is triggered. But the latch-up and wind-up issues may happen, which can challenge the recovery process [12]. Besides, another typical current limiting method is adding a virtual impedance between the inverter and the grid [13]-[15]. When the value of the virtual impedance is large enough, the output current of the inverter can be limited. However, tuning the virtual impedance in different cases (e.g. transient and steady states) may increase the control complexity.

Different from existing methods, this paper proposes a new idea called "power angle limit", which can guarantee that the power synchronization control law is still satisfied when the overcurrent protection is triggered. Since limiting the power angle is more reasonable than directly limiting the current, the stability of GFM inverters can be improved by using the proposed method. Moreover, considering that the real power angle is usually unknown, an equivalent virtual power angle is used for implementing the power limitation. Same as [16], this paper mainly focuses on the overcurrent condition caused by the overload. Simulation results show that the proposed power angle limiting method is effective under both strong and weak grid conditions.
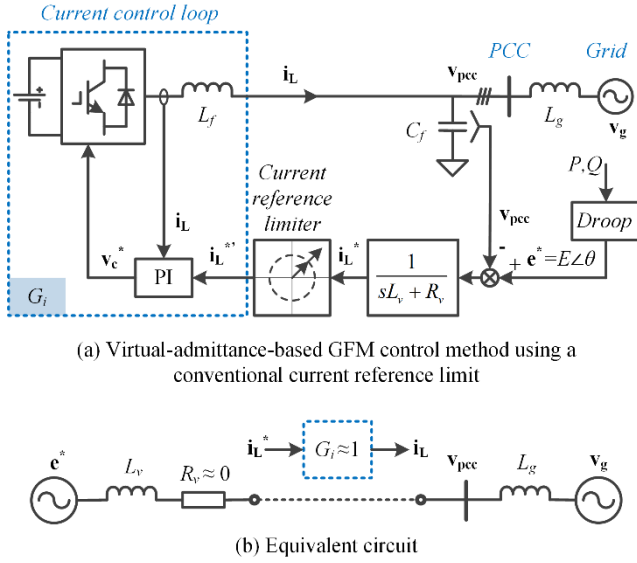
(a) Virtual-admittance-based GFM control method using a conventional current reference limit

(b) Equivalent circuit

Fig. 1. Virtual-admittance-based GFM inverter with a conventional current reference limiting method.

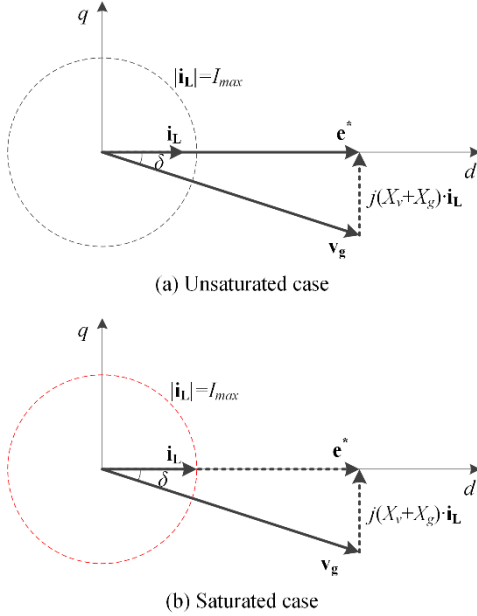(a) Unsaturated case

(b) Saturated case

Fig. 2. Voltage vector diagrams of GFM inverter in unsaturated and saturated cases.

The rest of this paper is organized as follows. Section II discusses the instability mechanism of the conventional current reference limiting method. Section III introduces a new power angle limiting method. Then, simulation results are presented in Section IV. Finally, this paper is concluded in Section V.

II. THEORETICAL ANALYSIS OF INSTABILITY MECHANISM OF CONVENTIONAL CURRENT REFERENCE LIMITING METHOD

A. Configurations of Typical Virtual Admittance-Based Grid-Forming Inverter Control Scheme

The schematic diagram of the virtual-admittance-based GFM inverter with the conventional current reference limiting

method is shown in Fig. 1. In Fig. 1(a), L_f and C_f are the filter inductor and capacitor. L_g is the grid inductor. $\mathbf{v_g}$ is the grid voltage, and $\mathbf{v_{pcc}}$ is the voltage at the point of common coupling (PCC). $\mathbf{i_L}$ is the current through the filter inductor. P and Q are the active and reactive power at the PCC. Moreover, the control system is performed in the synchronous rotating d-q frame (the voltage reference $\mathbf{e}^*$ is aligned to the d-axis). Notably, the coordinate transformation among different frames (i.e. a-b-c, α-β, and d-q) are omitted. The inner current control loop is a standard current control loop with the proportional-integral (PI) controller, which is the same as that in the conventional GFL inverter. The virtual admittance is equal to "1 / $(sL_v + R_v)$", where L_v is a virtual inductor and R_v is a virtual resistor. The droop controllers are typical P-f and Q-V droop controllers [17], [18]. In addition, the equivalent circuit of the GFM inverter system is shown in Fig. 1(b), where the filter capacitance C_f and the virtual resistance R_v are ignored because they are relatively small.

As shown in Fig. 1(a), a limiter is used to limit the current reference directly, where the limiting value is set as the maximum value (1 p.u.). When the magnitude of the current reference is lower than 1 p.u. (normal conditions), the current limiter is unsaturated. Thus, $\mathbf{i_L}^{*'}$ is equal to $\mathbf{i_L}^*$. However, when the magnitude of the current reference is higher than 1 p.u. (overcurrent conditions), the current limiter is saturated. Thus, the magnitude of $\mathbf{i_L}^{*'}$ is equal to 1 p.u. [10].

B. Instability Mechanism of the Current Reference Limiting Method

Same as [11], to simplify the analysis, it is assumed that the current vector $\mathbf{i_L}$ and the voltage vector $\mathbf{e}^*$ are in the same direction ideally. Thus, the voltage vector diagrams of the grid-connected system are shown in Fig. 2. As shown in Fig. 2(a), when the current limiter is unsaturated, the output power of the GFM inverter depends on two voltage vectors $\mathbf{e}^*$ and $\mathbf{v_g}$. In this case, the power meets the well-known power angle equation given by (1).

$$P = \frac{3}{2} \cdot \frac{E^* \cdot V_g}{X_v + X_g} \cdot \sin(\delta) \tag{1}$$

where E^* and V_g are the magnitudes of the vectors $\mathbf{e}^*$ and $\mathbf{v_g}$.

Moreover, as shown in Fig. 2(b), when the current limiter is saturated, the GFM inverter can be considered as a current source with a constant current magnitude. Thus, the output power of the GFM inverter depends on vectors $\mathbf{i_L}$ and $\mathbf{v_g}$. In this case, equation (1) is not satisfied anymore. Instead, the expression of the output power can be rewritten as (2) [11]. It is worth mentioning that when the directions of $\mathbf{i_L}$ and $\mathbf{e}^*$ are different, the analysis is more complicated. So, only the ideal case is considered here for qualitative analysis.

$$P = \frac{3}{2} \cdot I_{max} \cdot V_g \cdot \cos(\delta) \tag{2}$$

According to (1) and (2), theoretical operating trajectories of the GFM inverter by using different limiting methods are compared in Fig. 3.

(a) Without any limit

(b) With current reference limit
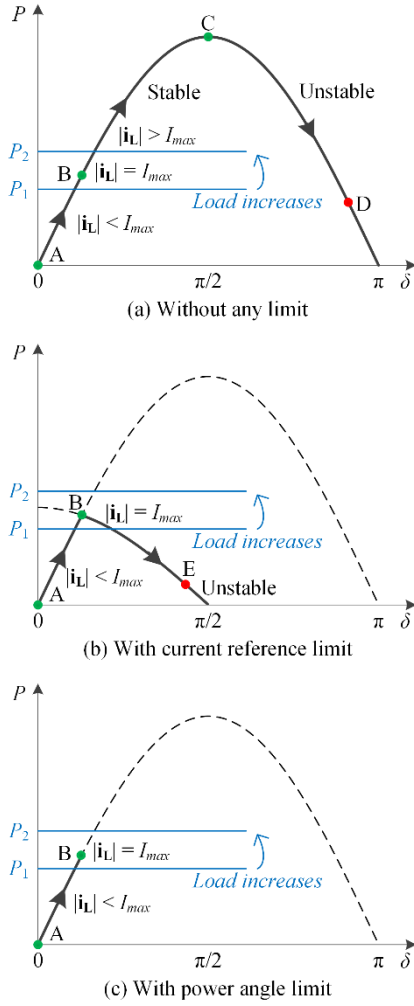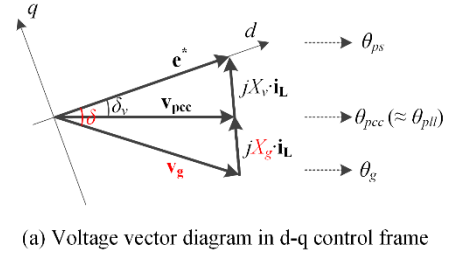

(c) With power angle limit

Fig. 3. Theoretical operating trajectories of GFM inverter with different current limiting methods under strong grid conditions.

Fig. 3(a) shows the trajectory of the GFM inverter without any limit. It can be seen that the trajectory follows the power angle curve A-B-C-D. It is assumed that the current magnitude reaches the maximum value I_{max} at the point B. Thus, when the load increases from P_1 to P_2, the output current of the inverter is higher than I_{max}, which is above the limit (overcurrent operation). Differently, Fig. 3(b) shows the trajectory of the GFM inverter with the current reference limit, which follows the curve A-B-E. When the load increases from P_1 to P_2, the current limiter is triggered. Thus, the trajectory moves from point B to point E, which finally leads to an unstable result [11]. To solve the instability problem caused by the current reference limit, a new idea of the power angle limit is proposed in this paper, which is shown in Fig. 3(c). If the power angle can be limited, the trajectory can stay at point B in overcurrent conditions.
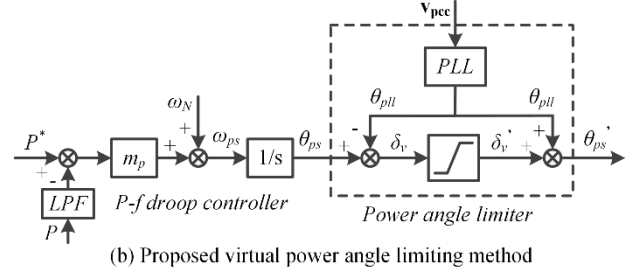
III. POWER ANGLE LIMITING METHOD AND ANALYSIS

A. Proposed Power Angle Limiting Method

To implement the idea of the power angle limit, the voltage vector diagram of the virtual-admittance-based GFM control method is shown in Fig. 4(a). Besides, the implementation of the proposed power angle limiting method is shown in Fig. 4(b).

(a) Voltage vector diagram in d-q control frame

(b) Proposed virtual power angle limiting method

Fig. 4. Implementation of the proposed power angle limiting method.

As shown in Fig. 4(a), considering the grid voltage $\mathbf{v_g}$ and grid inductance X_g are usually unknown, the real power angle δ is unknown. Thus, the power angle δ cannot be directly used for implementing the power limitation. Although the real power angle δ is unknown, the angle δ_v between the PCC voltage $\mathbf{v_{pcc}}$ and the reference voltage $\mathbf{e}^*$ is known, which is equal to (θ_{ps} - θ_{pcc}). Notably, the angle θ_{ps} is the phase angle of the vector $\mathbf{e}^*$, which is generated by the P-f droop controller. Besides, the angle θ_{pcc} is the phase angle of the vector $\mathbf{v_{pcc}}$, which can be estimated by the phase-locked loop (PLL). Namely, the angle θ_{pcc} is approximately equal to the PLL output angle θ_{pll}. Considering the PLL dynamics, the bandwidth of the PLL should be high enough to minimize the error (θ_{pll} - θ_{pcc}). Since the virtual power angle δ_v is also proportional to the active power, it is reasonable to limit the output power by limiting the angle δ_v. Therefore, the proposed virtual power angle limiting method is shown in Fig. 4(b). Notably, under normal conditions, δ_v is equal to δ_v' and δ_{ps} is equal to δ_{ps}'. Thus, the proposed power angle limiter does not have any additional influence under normal conditions. In other words, the proposed power angle limiter only works under overcurrent conditions.

According to the voltage vector diagram in Fig. 4(a), the relationship between the active power P and the virtual power angle δ_v meets an equivalent power angle equation:

$$P = \frac{3}{2} \cdot \frac{E^* \cdot V_{pcc}}{X_v} \cdot \sin(\delta_v) \qquad (3)$$

Then, the virtual power angle δ_v can be calculated as:

$$\delta_v = \arcsin(\frac{2}{3} \cdot \frac{P \cdot X_v}{E^* \cdot V_{pcc}}) \qquad (4)$$

Thus, when the limiting value of the active power P is determined (e.g. 0.9 p.u.), the limiting value of the virtual power angle δ_v can be obtained according to (4).
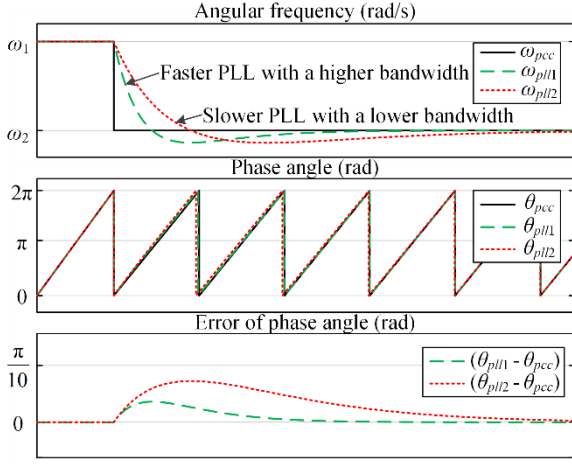
Fig. 5. Error of phase angle estimation when considering PLL dynamics.

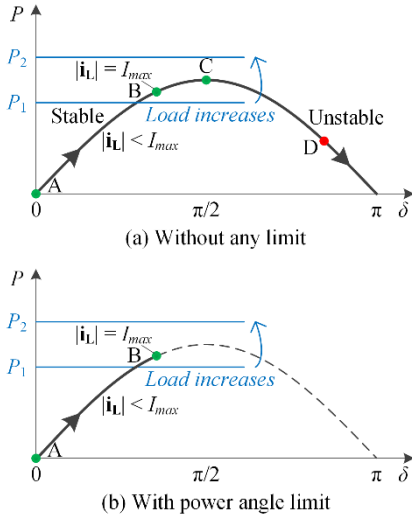(a) Without any limit

(b) With power angle limit

Fig. 6. Theoretical operating trajectories of GFM inverter with different current limiting methods under weak grid conditions.

B. Discussion of PLL Dynamics

As aforementioned, the proposed power angle limiting method introduces a PLL to estimate the phase angle of the PCC voltage. However, an inaccurate phase angle estimation may lead to uncertain performance. Hence, the impact of the PLL dynamics on the proposed method needs to be discussed.

The theoretical analysis of the PLL dynamics is presented in Fig. 5, where a faster PLL and a slower PLL are compared. It can be seen in Fig. 5 that when the angular frequency of the PCC voltage is reduced from ω_1 to ω_2, the frequency dynamic responses of the two PLLs are different, and the errors of the phase angle estimation are different. Obviously, the error of the phase angle by using the faster PLL is smaller. Therefore, a fast PLL with a high bandwidth is used in this paper.

Notably, it is known that a fast PLL may worsen the small-signal stability of GFL inverters under weak grid conditions [19], [20]. Similarly, the proposed method with a fast PLL may also have some unexpected results under ultra-weak grids, which is worth being studied further in the future.

Parameters	Values
Grid phase voltage (peak value), V_g	311 V (1 p.u.)
Rated voltage of inverter, V_N	311 V (1 p.u.)
Rated angular frequency, ω_N	2π·50 rad/s (1 p.u.)
Rated active power of inverter, P_N	30 kW (1 p.u.)
Maximum current of inverter, I_{max}	64.3 A (1 p.u.)
DC-link voltage, V_{dc}	700 V
Output filter inductor, L_f	3 mH (0.2 p.u.)
Output filter capacitor, C_f	10 μF (0.015 p.u.)
Short circuit ratio, SCR	30 ~ 1.2
Grid inductor, L_g	0.5 ~ 12.8 mH
Sampling frequency, f_s	10 kHz
Designed current-loop bandwidth, ω_i	2000 rad/s
Virtual inductance, L_v	7.65 mH (0.5 p.u.)
Virtual resistance, R_v	0.24 Ω (0.05 p.u.)
Output power limiting value, P_{lim}	27 kW (0.9 p.u.)
Active power droop coefficient, m_p	2.5%·ω_N/P_N
Reactive power droop coefficient, n_q	5%·V_N/P_N
Damping ratio of PLL, ζ	1
Natural angular frequency of PLL, ω_n	200 rad/s

C. Analysis of the Weak Grid Conditions

According to the power angle equation in (1), as the grid inductance X_g increases, the maximum value of the power angle curve will decrease, which may reduce the stability margin of the system. Therefore, the weak grid condition is a worse case for the grid-connected inverters, which will be analyzed in this section.

Different from the strong grid conditions, the theoretical operating trajectories of the GFM inverter under weak grid conditions are shown in Fig. 6, where point B is closer to point C. Fig. 6(a) shows the trajectory of the GFM inverter without any limit, which follows the power angle curve A-B-C-D. It is assumed that the current magnitude reaches the maximum value I_{max} at the point B. Thus, when the load increases from P_1 to P_2, the output current of the inverter is higher than I_{max}. Besides, when the load power P_2 is higher than the maximum value of the power angle curve (point C), the trajectory moves from point B to points C and D. Finally, the system becomes unstable. Notably, even when the current reference limiting method is used, the instability problem still exists, which has been analyzed in the previous section. Hence, this method is not effective. Differently, as shown in Fig. 6(b), when the proposed power angle limiting method is used, the trajectory can stay at point B under the overcurrent conditions. Thus, the proposed method not only limits the output current of the GFM inverters but also improves the transient stability of the GFM inverters under weak grid conditions.
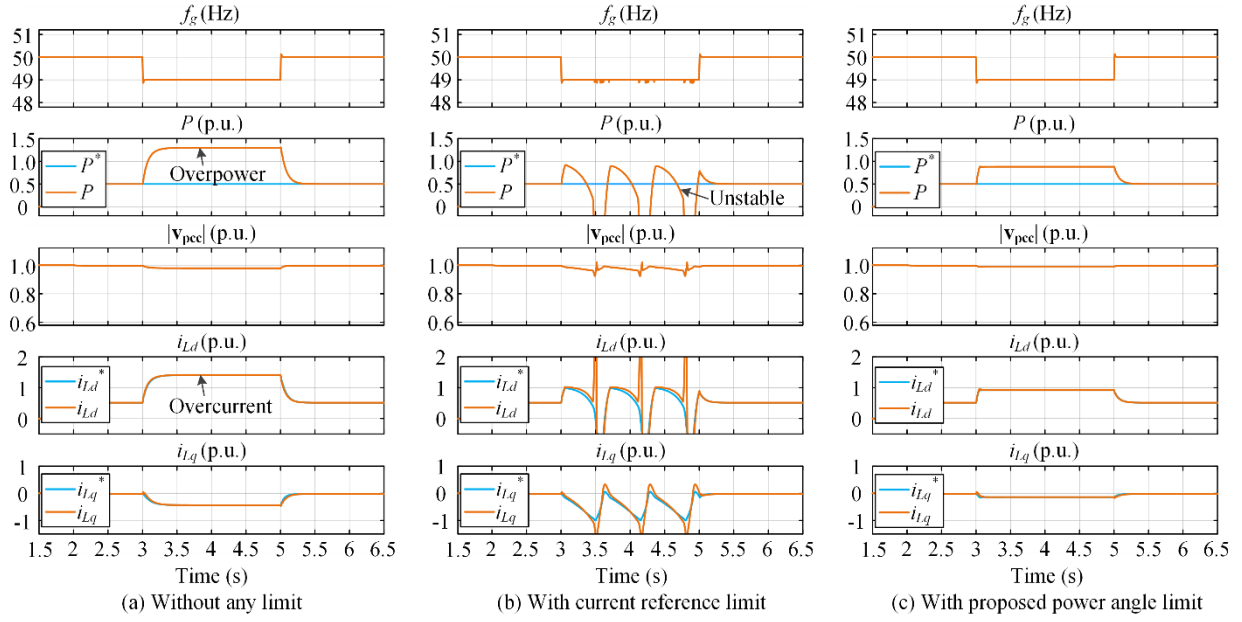
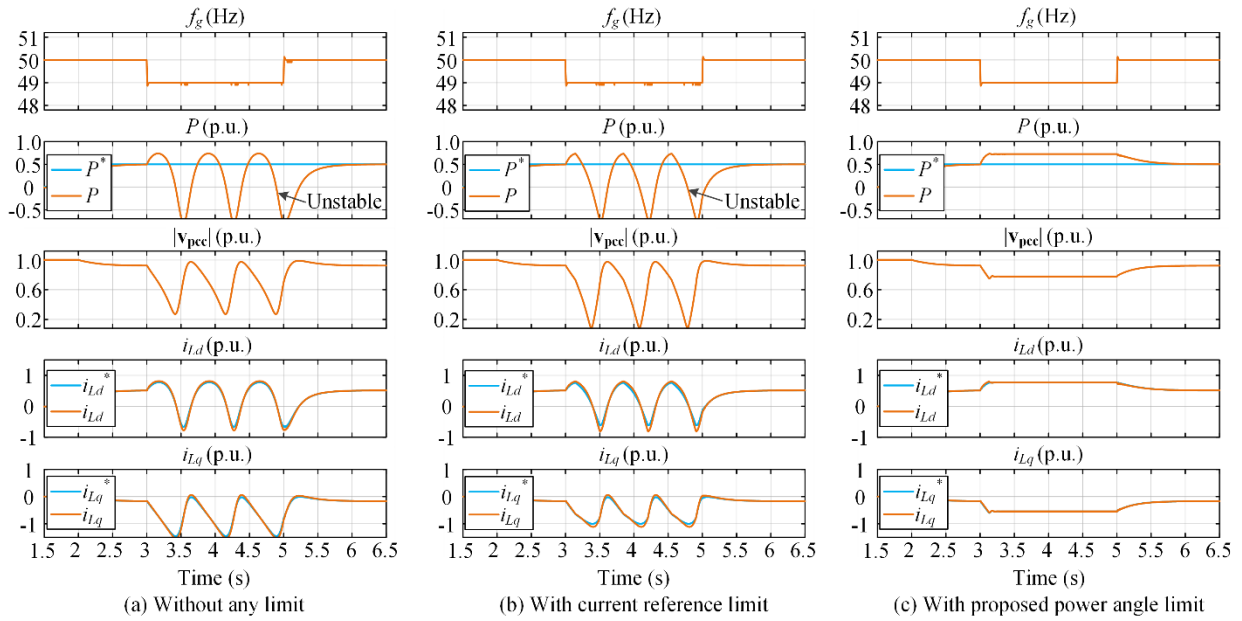Fig. 7. Simulation results of different current limiting methods under strong grid conditions (SCR = 30).

Fig. 8. Simulation results of different current limiting methods under weak grid conditions (SCR = 1.2).

D. Windup Issue of the Proposed Power Angle Limiter

It can be seen from Fig. 4 that when the power angle limiter is triggered, the output angle of the limiter θ_{ps}' does not depend on the P-f droop controller anymore. However, the integrator in the P-f droop controller still works. Thus, the windup issue of the integrator is worth being discussed.

It can be seen from Fig. 4(b) that when the power angle limiter is triggered, the output angle θ_{ps}' mainly depends on θ_{pll}, which means that only using the PLL is enough to keep synchronization with the grid. To avoid the windup issue of the P-f droop controller, the integrator in the P-f droop controller can be disabled when the limiter is saturated. Then, when the

limiter is out of saturation, the integrator can be enabled. Thus, the GFM inverter can return to the normal operation smoothly.

IV. SIMULATION RESULTS

In order to verify the effectiveness of the proposed power angle limiting method, a 30 kW virtual admittance based GFM inverter simulation model is established in Matlab/Simulink. The system and control parameters are shown in Table I. To avoid the influence of the high-frequency harmonics, an average model of the inverter is used. Besides, a strong grid condition with SCR = 30 and a weak grid condition with SCR = 1.2 are used as examples to test the performance of the proposed

method. Simulation results with different limiting methods are compared in Fig. 7 and Fig. 8.

Fig. 7 shows the simulation results under the strong grid condition with SCR = 30. It can be seen from Fig. 7(a) that when the grid frequency is reduced from 50 Hz to 49 Hz, both the output power and current are higher than 1 p.u. Besides, as shown in Fig. 7(b), when the current reference limiting method is used, the system becomes unstable under overcurrent conditions. Differently, as shown in Fig. 7(c), when the proposed power angle limiting method is used, the system is stable under overcurrent conditions.

Comparing the simulation results in Fig. 7(a)-(c), it can be seen that the proposed method can improve the stability of the GFM inverters under overcurrent conditions in the strong grid. Moreover, the simulation results in Fig. 7 agree well with the theoretical analysis in Fig. 3, which proves the correctness of the theoretical analysis. In addition, Fig. 8 shows the simulation results under the weak grid condition with SCR = 1.2. It can be seen from Fig. 8(a) that when the grid frequency is reduced from 50 Hz to 49 Hz, the system becomes unstable in the case without any limit. Besides, as shown in Fig. 7(b), when the current reference limiting method is used, the system is also unstable under overcurrent conditions. So, this method is not effective. Differently, as shown in Fig. 7(c), when the proposed power angle limiting method is used, the system is stable under overcurrent conditions. Therefore, the proposed method can improve the stability of the GFM inverters under overcurrent conditions in the weak grid. The simulation results in Fig. 8 are in accordance with the theoretical analysis in Fig. 6.

Furthermore, as shown in Fig. 7(c) and Fig. 8(c), when the grid frequency is changed back to 50 Hz, the GFM inverter with the proposed method can return to the normal operation mode smoothly in both strong and weak grids. Therefore, the anti-windup scheme is effective.

V. Conclusion

Aiming at the instability issue caused by the conventional current reference limiting method, this paper proposes a new idea of limiting the power angle. Considering that the real power angle is usually hard to obtain, an equivalent virtual power angle is used for implementing the power limitation. Since the power synchronization control law is still satisfied when the proposed power angle limiter is triggered, the stability of GFM inverters under the overcurrent conditions can be guaranteed. Thus, the instability issue of the GFM inverters under overcurrent conditions caused by the overload has been solved. Finally, simulation results of the GFM inverters with the proposed power angle limiting method show good stability and transient performance in both strong and weak grids. Furthermore, it is worth mentioning that the current limitation during the low-voltage ride-through is another challenge for GFM inverters, which will be investigated in the future.

References

[1] "GC0137: Minimum specification required for provision of GB grid forming (GBGF) capability," *National Grid ESO*, Dec. 2021.

[2] U. Markovic, O. Stanojev, P. Aristidou, E. Vrettos, D. Callaway and G. Hug, "Understanding small-signal stability of low-inertia systems," *IEEE Trans. Power Syst.*, vol. 36, no. 5, pp. 3997-4017, Sep. 2021.

[3] R. Rosso, X. Wang, M. Liserre, X. Lu and S. Engelken, "Grid-forming converters: control approaches, grid-synchronization, and future trends - A review," *IEEE Open J. Ind. Appl.*, vol. 2, pp. 93-109, 2021.

[4] S. D'Arco and J. A. Suul, "Virtual synchronous machines - classification of implementations and analysis of equivalence to droop controllers for microgrids," *IEEE Gren. Conf.*, pp. 1-7, 2013.

[5] H. Bevrani, T. Ise, and Y. Miura, "Virtual synchronous generators: a survey and new perspectives," *Electr. Power Energy Syst.*, vol. 54, pp. 224-254, 2014.

[6] W. Du, Z. Chen, K. P. Schneider, R. H. Lasseter, S. P. Nandanoori, F. K. Tuffner, et al., "A comparative study of two widely used grid-forming droop controls on microgrid small-signal stability," *IEEE J. Emerg. Sel. Top. Power Electron.*, vol. 8, no. 2, pp. 963-975, Jun. 2020.

[7] P. Rodriguez, I. Candela, C. Citro, J. Rocabert and A. Luna, "Control of grid-connected power converters based on a virtual admittance control loop," *15th Europ. Conf. Power Electron. Appl. (EPE)*, pp. 1-10, 2013.

[8] L. Huang, C. Wu, D. Zhou and F. Blaabjerg, "Impact of virtual admittance on small-signal stability of grid-forming inverters," *6th IEEE Workshop Electron. Grid (eGRID)*, pp. 1-8, 2021.

[9] A. Tarraso, N.-B. Lai, G.N. Baltas, and P. Rodriguez, "Power quality services provided by virtually synchronous FACTS," *Energies*, vol. 12, no. 17, pp. 3292, Aug. 2019.

[10] M. G. Taul, X. Wang, P. Davari and F. Blaabjerg, "Current limiting control with enhanced dynamics of grid-forming converters during fault conditions," *IEEE J. Emerg. Sel. Top. Power Electron.*, vol. 8, no. 2, pp. 1062-1073, Jun. 2020.

[11] H. Xin, L. Huang, L. Zhang, Z. Wang and J. Hu, "Synchronous instability mechanism of P-f droop-controlled voltage source converter caused by current saturation," *IEEE Trans. Power Syst.*, vol. 31, no. 6, pp. 5206-5207, Nov. 2016.

[12] T. Liu, X. Wang, F. Liu, K. Xin and Y. Liu, "A current limiting method for single-loop voltage-magnitude controlled grid-forming converters during symmetrical faults," *IEEE Trans. Power Electron.*, vol. 37, no. 4, pp. 4751-4763, April 2022.

[13] A. D. Paquette and D. M. Divan, "Virtual impedance current limiting for inverters in microgrids with synchronous generators," *IEEE Trans. Ind. Appl.*, vol. 51, no. 2, pp. 1630-1638, Mar.-Apr. 2015.

[14] A. Gkountaras, S. Dieckerhoff and T. Sezi, "Evaluation of current limiting methods for grid forming inverters in medium voltage microgrids," *IEEE Energy Conv. Cong. Exp. (ECCE)*, pp. 1223-1230, 2015.

[15] E. Rokrok, T. Qoria, A. Bruyere, B. Francois and X. Guillaud, "Transient stability assessment and enhancement of grid-forming converters embedding current reference saturation as current limiting strategy," *IEEE Trans. Power Syst.*, vol. 37, no. 2, pp. 1519-1531, Mar. 2022.

[16] W. Du, R. H. Lasseter and A. S. Khalsa, "Survivability of autonomous microgrid during overload events," *IEEE Trans. Smart Grid*, vol. 10, no. 4, pp. 3515-3524, Jul. 2019.

[17] S. Wang, Z. Liu, J. Liu, D. Boroyevich and R. Burgos, "Small-signal modeling and stability prediction of parallel droop-controlled inverters based on terminal characteristics of individual inverters," *IEEE Trans. Power Electron.*, vol. 35, no. 1, pp. 1045-1063, Jan. 2020.

[18] H. Wu and X. Wang, "Small-signal modeling and controller parameters tuning of grid-forming VSCs with adaptive virtual impedance-based current limitation," *IEEE Trans. Power Electron.*, vol. 37, no. 6, pp. 7185-7199, Jun. 2022.

[19] B. Wen, D. Boroyevich, R. Burgos, P. Mattavelli and Z. Shen, "Analysis of D-Q small-signal impedance of grid-tied inverters," *IEEE Trans. Power Electron.*, vol. 31, no. 1, pp. 675-687, Jan. 2016.

[20] L. Huang, C. Wu, D. Zhou and F. Blaabjerg, "A double-PLLs-based impedance reshaping method for extending stability range of grid-following inverter under weak grid," *IEEE Trans. Power Electron.*, vol. 37, no. 4, pp. 4091-4104, Apr. 2022.